Vol. 78 No. 1 ACTA GEOLOGICA SINICA Feb. 2004 131–136
http://www.geojournals.cn/dzxbcn/ch/index.aspx

Underplating of Mesozoic Mantle-derived Magmas in Tongling, Anhui Province: Evidence from Megacrysts and Xenoliths

DU Yangsong[1, 2], LEE Hyunkoo[3] and QIN Xinlong[2]
1 *Key Laboratory of Lithosphere Tectonics and Exploration, Ministry of Education, 29 Xueyuan Road, Beijing 100083; E-mail: ysdu@cugb.edu.cn*
2 *Faculty of Earth Sciences and Mineral Resources, China University of Geosciences, 29 Xueyuan Road, Beijing 100083*
3 *Department of Geology, Chungnan National University, 220 Kungdong, Yuseong Ku, Taejon 305-764, Republic of Korea*

Abstract Lithological observations and mineralogical analyses on pyroxene and hornblende megacrysts and pyroxene and hornblende cumulates in xenoliths in the Mesozoic plutons of the Tongling region, Anhui Province, provide evidence for the magmatic underplating of mantle-derived alkali-olivine basalt at circa 140 Ma. The pyroxene and hornblende megacrysts and cumulates were formed through the AFC process at depths ranging from 27 to 35 km.

Key words: magma underplating, megacrysts, xenoliths, Tongling in Anhui Province

1 Introduction

Underplating of mantle-derived magmas plays a major role in crust-mantle interaction, affecting a wide range of geological processes, including basin formation, crust accretion, magmatic evolution, fluid transportation, regional metamorphism and regional mineralization (Du et al., 2003). In addition to regional geological mapping and field investigation, methods in such disciplines as seismology, petrology, geochemistry and geothermics, especially enclave petrology and geochemistry, have all contributed to our understanding of mantle-derived magma underplating. Most of attention in previous studies of magma underplating based on enclave petrology and geochemistry has focused on granulite xenoliths in basic lava (Zhou et al., 1992; Xu et al., 1995; Fan et al., 1996; 1998; 2001; Yu et al., 1998; 2002; Sachs et al., 2000; Zheng et al., 2001), while less attention has been paid to the data from xenoliths in felsic or intermediate-basic intrusive rocks (Shao et al., 1999, 2000).

Magmatic activity was intense during the Mesozoic in the middle segment of the Yangtze magmatic-metallogenic belt of Tongling, Anhui Province, and formed many plutons. A wide variety of megacrysts and xenoliths occur in these plutons, of which pyroxene and hornblende megacrysts and pyroxene and hornblende cumulates is studied in detail this time. This paper summarizes the characteristics of these megacrysts and xenoliths and discusses their implications on the Mesozoic mantle-derived magma underplating in the Tongling region, Anhui Province.

2 Petrography

Pyroxene and hornblende megacrysts occur in the Caoshan porphyritic pyroxene diorite pluton. The pyroxene megacrysts range from 0.6 to 1.0 cm in size, and are fractured (Plate 1). Fractures on the margins of some pyroxene megacrysts are filled up with minerals of host rock. The hornblende megacrysts range from 0.5 to 3.1 cm in diameter. Corrosion or alteration associated with fractures is common along the margins of the hornblende megacrysts (Plate 2).

Pyroxene cumulates are mainly exposed in the Caoshan pluton of pyroxene monzodioritic and pyroxene dioritic porphyritic rocks. They are composed of clinopyroxene (80–90%) and hornblende (5–15%), with minor magnetite and pyrite, and local coarse-grained apatite. The rocks have typical cumulate and occasional mosaic textures. The enclaves and the host rocks have distinct contacts and the margins of the formers are sometimes broken up by the magma of the latter (Plate 3).

Hornblende cumulates occur in felsic and intermediate-basic plutons, especially in the Jiguanshi granodioritic and Caoshan pyroxene dioritic porphyritic plutons. Hornblende cumulates have typical cumulate and mosaic textures (Plate 4) and consist mainly of hornblende (90–95%) with minor apatite (2–6%) and clinopyroxene (1–2%) as well as traces

of epidote and magnetite. The pyroxenes lack distortion or exsolution, and occur as residual crystals in hornblendes. Chloritization or biotitization of the hornblendes occurs along the contact zone between the cumulate and the host.

3 Mineral Chemistry and Estimation of Equilibrium Pressure and Temperature

Mineral compositions were determined with a Superprobe 733 type electronprobe at the China University of Geosciences, Beijing. Compositions of pyroxenes and hornblendes in the megacrysts and cumulates are listed in Table 1. The analyses were completed with an accelerating voltage of 15 kV and sample electric current of 0.02 mA. Natural minerals were selected as the standard samples during the calibration and actual analyses. Cation numbers of pyroxenes and hornblendes were counted based on 6 oxygens and 23 oxygens, respectively, and the Fe^{3+} contents were calculated separately by both the end-member molecular proportion matching procedure (Zheng, 1984) and the average potential difference value method proposed by Ye (1992). Compositions of megacrystalline hornblendes in alkali-olivine basalts in typical regions of East China (Chi, 1987) are included in Table 1 for comparison.

Clinopyroxenes are rich in calcium (CaO= 21.84–23.34%) and belong to salites of calcareous pyroxenes. Compositionally, all samples are similar to phenocrysts of pyroxenes from alkali-olivine basalts in the typical regions of East China (Chi, 1987), except for those from the Jiguanshi hornblende cumulates which have a relatively high content of Al_2O_3 (5.32–5.93%), and a low content of SiO_2 (48.57–49.37%) and MgO (2.48–12.67%). In a plot of Al^{IV} vs. Al^{VI} for clinopyroxenes (Qiu et al., 1991), all data are plotted in the field of phenocryst and microlite clinopyroxene in basalts determined by Warren (1979), of which those of the pyroxenes from the Jiguanshi hornblende cumulates also fall in the field of high-pressure facies clinopyroxenes determined by Qiu et al. (1987) (Fig. 1).

Hornblendes all show $Ca_B \geq 1.50$, $(Na+K)_A \geq 0.50$, Si > 5.5 but < 6.5, Ti < 0.5, $Mg/(Mg+Fe^{2+}) > 0.5$, and $Al^{VI} > Fe^{3+}$, and have a high content of CaO (11.06–12.29%) and Al_2O_3 (13.57–14.39%), thus are classified as pargasite

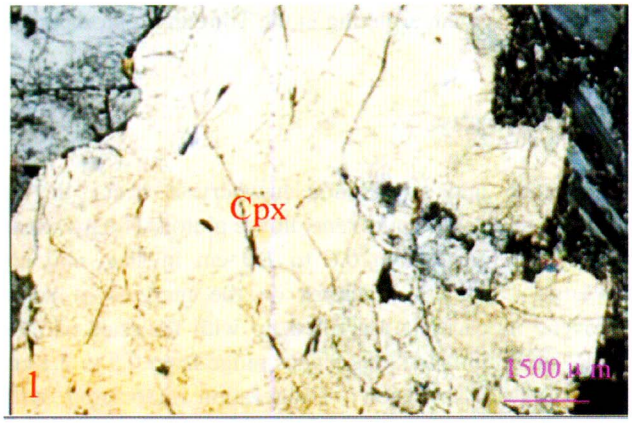

Plate 1. A clinopyroxene megacryst with internal fractures and a resorption border. Caoshan pluton, crossed polars.

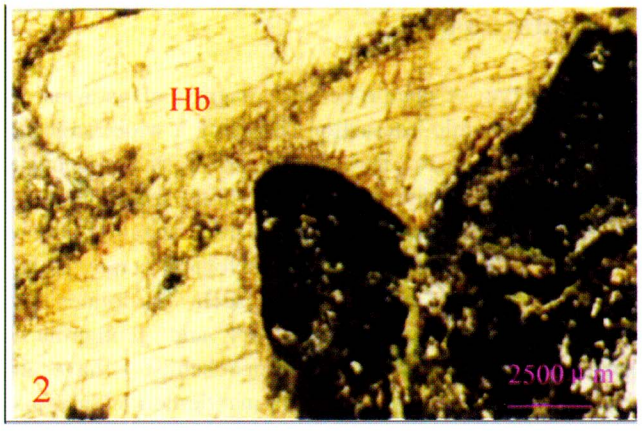

Plate 2. A hornblende megacryst with a resorption border. Caoshan pluton, crossed polars.

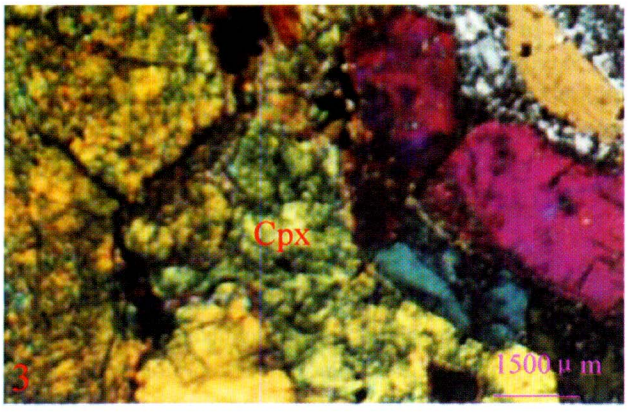

Plate 3. Pyroxene cumulate. Caoshan pluton, crossed polars.

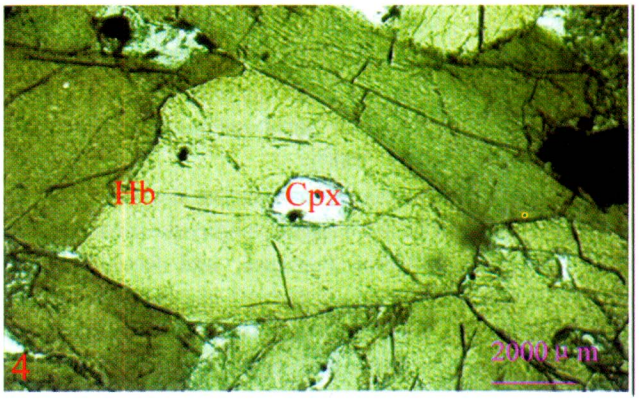

Plate 4. Hornblende cumulate with mosaic texture and clinopyroxene occurring in hornblende as residual crysts without kink bands or exsolution. Jiguanshi, crossed polars.

Table 1 Electron-probe analyses of minerals

Pluton	Sample type	Sample No.	Mineral	SiO_2	$Ti O_2$	Al_2O_3	Cr_2O_3	Fe_2O_3	FeO	MnO	MgO	CaO	Na_2O	K_2O	NiO	P_2O_5	Total
Caoshan	Pyroxenitic cumulate	CS-12-6	Pyroxene	48.68	1.39	4.27	0.16		7.81	0.11	15.05	21.84	0.47	0.05	0.10	0.25	99.93
Caoshan	Pyroxene megacryst	CS-3-2-1	Pyroxene	50.6	0.79	4.37			7.70	0.18	13.93	22.64	0.54	0.14			100.89
Caoshan	Pyroxene megacryst	CS-3-2-6	Pyroxene	50.16	0.63	4.74			7.49	0.16	14.32	22.88	0.32	0.00			100.7
Jiguanshi	Hornblenditic cumulate	JGSH-11-3-2	Pyroxene	49.37	0.86	5.93			7.12	0.17	12.48	23.34	0.66	0.00			99.93
Jiguanshi	Hornblenditic cumulate	JGSHA-21-2	Pyroxene	48.57	1.25	5.32	0.15		7.28	0.35	12.67	21.87	0.18	0.00	0.44	0.65	98.73
Jiguanshi	Hornblenditic cumulate	JGSH-11-3-1	Hornblende	42.25	2.91	14.39	0.02		11.29	0.05	12.66	12.29	1.93	1.14			98.93
Caoshan	Hornblende megacryst	CS-7-10	Hornblende	40.14	2.57	13.73			12.21	0.15	12.89	11.95	2.20	1.49			97.33
Caoshan	Hornblenditic cumulate	CS-hbd-2	Hornblende	41.15	2.61	13.94			13.95	0.03	11.46	11.06	2.54	1.25		0.31	98.3
Caoshan	Hornblende megacryst	CS-3-1-2	Hornblende	41.2	2.89	14.17			13.13	0.01	12.52	11.66	1.93	1.17			98.68
Jiguanshi	Hornblenditic cumulate	JGSHA-21-4	Hornblende	40.83	2.4	13.57			13.09	0.14	12.06	11.29	1.68	1.08	0.03	0.29	96.46
Puning*	Hornblende megacryst	1-4	Hornblende	39.74	2.99	14.25	0.08	5.96	7.41	0.14	13.29	10.88	2.15	1.40	0.01	0.09	98.39
Caoshan	Hornblende megacryst	CS-7z-4	Hornblende	39.48	2.32	14.34	0.27		12.57	0.05	12.81	11.56	2.18	1.16	0.13	0.43	97.3
Jiguanshan	Hornblende megacryst	JGSB-2-1	Hornblende	39.66	2.91	14.37			12.37	0.34	12.44	11.75	2.40	0.80			97.04
Huinan*	Hornblende megacryst	6-7	Hornblende	40.18	6.18	15.2	0.06		10.14	0.05	11.92	9.78	30..	1.55			95.06
Arizona*	Hornblende megacryst	8-9	Hornblende	40.78	4.32	15.26			10.14	0.09	12.67	10.36	2.96	1.53			98.11
Pingquan*	Hornblende megacryst	5	Hornblende	39.86	1.36	15.46		6.19	12.14	0.02	6.99	9.08	3.04	1.99	0.00	0.30	96.43

Sample No.	Si	Ti	Al	Cr	Fe^{+3}	Fe^{+2}	Mn	Mg	Ca	Na	K	*P* (kPa) **	*D* (km)	*T* (℃)	Al^{IV}	Al^{VI}	Name
CS-12-6	1.796	0.039	0.186	0.005	0.176	0.068	0.003	0.828	0.863	0.034	0.002	8.83	29.1	1131	0.186	0.000	Augite
CS-3-2-1	1.854	0.022	0.189	0.000	0.105	0.131	0.006	0.761	0.889	0.038	0.007	9.02	29.8	1133	0.146	0.043	Salite
CS-3-2-6	1.839	0.017	0.205	0.000	0.105	0.124	0.005	0.783	0.899	0.023	0.000	10.06	33.2	1145	0.161	0.044	Salite
JGSH-11-3-2	1.845	0.036	0.238	0.005	0.010	0.235	0.011	0.717	0.890	0.013	0.000	12.21	40.3	1169	0.155	0.083	Salite
JGSHA-21-2	1.829	0.024	0.259	0.000	0.083	0.137	0.005	0.689	0.926	0.047	0.000	13.57	44.8	1184	0.171	0.088	Salite
JGSH-11-3-1	6.152	0.272	2.410	0.000	0.000	1.653	0.018	2.709	1.832	0.493	0.209	8.83	29.1		1.848	0.562	Pargasite
CS-7-10	5.986	0.288	2.413	0.000	0.096	1.427	0.019	2.866	1.915	0.638	0.284	8.85	29.2		2.014	0.399	Pargasite
CS-hbd-2	6.115	0.292	2.441	0.000	0.000	1.734	0.004	2.539	1.766	0.734	0.238	9.01	29.7		1.885	0.556	Pargasite
CS-3-1-2	6.052	0.319	2.453	0.000	0.000	1.613	0.001	2.742	1.844	0.552	0.220	9.07	29.9		1.948	0.505	Pargasite
JGSHA-21-4	6.167	0.319	2.476	0.002	0.000	1.378	0.006	2.755	1.924	0.547	0.212	9.20	30.4		1.833	0.643	Pargasite
1-4	5.886	0.333	2.488	0.009	0.250	1.304	0.018	2.935	1.740	0.622	0.267	9.27	30.6		2.114	0.374	Pargasite
CS-7z-4	5.901	0.261	2.526	0.032	0.196	1.391	0.006	2.855	1.862	0.636	0.223	9.49	31.3		2.099	0.427	Pargasite
JGSB-2-1	5.923	0.327	2.529	0.000	0.069	1.476	0.043	2.770	1.888	0.698	0.153	9.50	31.4		2.077	0.452	Pargasite
6-7	5.971	0.476	2.633	0.000	0.000	1.242	0.011	2.765	1.628	0.842	0.286	10.09	33.3		2.029	0.604	Pargasite
8-9	5.909	0.684	2.635	0.007	0.000	1.247	0.006	2.614	1.542	0.856	0.291	10.10	33.3		2.091	0.544	Pargasite
5	6.014	0.154	2.754	0.000	0.707	1.531	0.009	2.020	1.467	0.888	0.386	10.77	35.5		1.986	0.768	Pargasite

* Data from Chi (1987), with 4 samples in Puning, 2 in Huinan, 2 in Arizona, and 1 in Pingquan; ** Temperature and pressure for crystallization of clinopyroxene were estimated by using the aluminum-in-clinopyroxene geothermometer and geobarometer after Qiu et al. (1987), and pressure for crystallization of hornblende by using the aluminum-in-hornblende geobarometer after Hollister, Grissom, Peters, Stowell and Gisson (1987).

based on the scheme proposed by IMA-CNMMN (1997). All megacrystalline hornblendes collected from the alkali olivine basalts in the typical regions of East China are also pargasite. In a plot of Ti vs. Al (Best, 1974), all data of hornblendes including those occurring as megacrysts in the alkali olivine basalts typical elsewhere in East China are plotted in the field of mantle-derived hornblende compositions (Fig. 2).

The forming temperature, pressure and depth of the megacrysts and cumulates including those in the alkali-olivine basalts in the typical regions of East China (see Table 1) were calculated by using the geothermometer and geobarometer of aluminum in clinopyroxene proposed by Qiu et al. (1987) and the geobarometer of aluminum in hornblende proposed by Hollister et al. (1987).

Based on the chemistry of clinopyroxenes in the Jiguanshi hornblende cumulates, the temperature of mineral crystallization at depths is estimated to be 1169–1184°C, and the corresponding pressure and depth are 12.21–13.57 kPa and 40–45 km, respectively. The temperature estimates of mineral crystallization at intermediate crustal levels based on pyroxene and hornblende mineral chemistry fall within the range of 1131–1145°C, with a corresponding pressure and depth range of 8.83–10.06 kPa and 29 – 33 km. These temperatures and pressures are identical to those determined on aluminum contents in the megacrysts in the alkali-olivine basalts elsewhere in East China.

4 Discussion and Conclusions

Geochronology of the hornblende and pyroxene cumulate xenoliths and their host rocks in the Jiguanshi pluton yielded Rb-Sr isochron ages of about 140 Ma with $(^{87}Sr / ^{86}Sr)_0 = 0.7067–0.7069$ (Tang et al., 1998).

Through comprehensive petrological, petrochemical, isotope geochemical and experiment petrological studies, Xing et al. (1996; 1997) suggested that the intrusive rocks in the Tongling region were formed by crystallization of the evolved magma, which was produced by assimilation of mantle-derived alkaline basaltic magma with felsic components of the Archean granulitic lower crust and intruded into shallower crust after fractionation of pyroxene, amphibole, magnetite and apatite.

The pyroxene and hornblende cumulates in Tongling have a typical cumulate texture and show broken margins caused by the host magma. The margins of pyroxene and hornblende megacrysts are generally corroded, and occasionally broken to several pieces with minerals of host rock being filled up in between. Alteration of hornblendes is common in the hornblende cumulates, and gets stronger as they are more close to the contact zones with the host

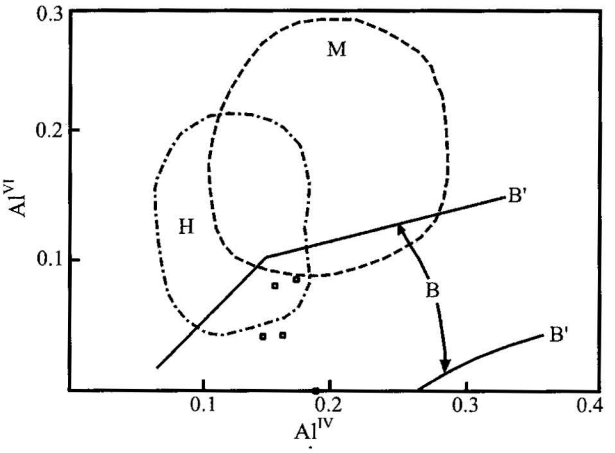

Fig. 1. Al^{IV} vs. Al^{VI} diagram for clinopyroxenes (after Qiu et al., 1991).
B (B'-B') – Low-pressure phase phenocrysts and microlite clinopyroxenes in basalt (Warren, 1979); M – medium-pressure phase megacrystalline clinopyroxences (based on 109 samples; H – high-pressure phase clinopyroxences (based on 183 samples) (Qiu et al., 1987).

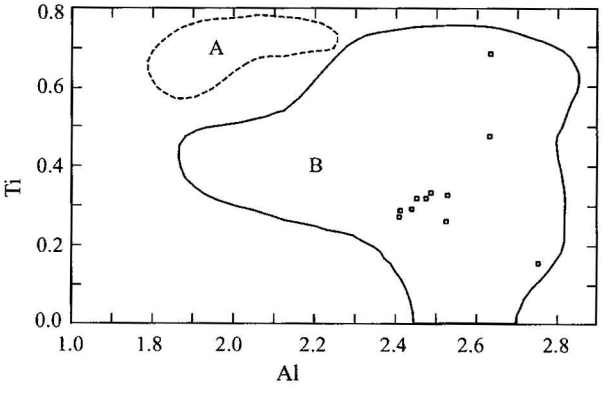

Fig. 2. Al vs. Ti diagram for hornblendes (after Best, 1974).
A – Megacrystalline; B – poikilitic.

rocks. These facts indicate that they were formed before the formation of their host rocks. Occurrence of the pyroxenes with no distortion or exsolution in the hornblende cumulates as residual crystals in hornblendes indicates that the pyroxenes were formed not by disintegration of mantle rocks, but by crystallization of basaltic magma before the formation of cumulating hornblendes. The compositions of the pyroxenes and hornblendes are similar to those of the phenocrystal pyroxenes and megacrystalline hornblendes collected from the alkali-olivine basalts in East China. In the diagram of Al^{IV} vs. Al^{VI} for clinopyroxene, all data are plotted in the field of phenocryst and microlite clinopyroxene in (alkali-olivine) basalts, of which those of the pyroxenes from the Jiguanshi hornblende cumulates also fall in the field of high-pressure facies clinopyroxenes. In a plot of Ti vs. Al (Best, 1974), all data of hornblendes including the megacrystalline ones collected from the alkali

olivine basalts in the typical regions of East China are plotted in the field of mantle-derived hornblende compositions. In addition, the crystallization temperature of the pyroxenes in the Jiguanshi hornblende cumulates ranges from 1169°C to 1184°C, and the corresponding depth from 40 to 45 km, while that of the pyroxenes and hornblendes from the other samples varies from 1128°C to 1145°C, and the corresponding depth from 27 to 35 km. These results are consistent with mineral crystallization of pyroxene and hornblende cumulates in the Baimangshan pyroxene monzodioritic pluton at up to 1130°C and 31 km estimated by Zhou et al. (1993) and Wu et al. (1997).

A deep seismic reflection profile survey revealed that a strong mantle-derived magma underplating along the Yangtze River in Anhui Province took place in the Mesozoic (Lü et al., 2003). It is inferred based on the combined geophysical and regional geological study (Chen, 1988; Lü et al., 2003) that the maximum Moho depth is about 32 km, and the minimum Moho depth is 30–31 km along the Yangtze River in Anhui Province.

Based on the facts mentioned above, it may be inferred that a continent-continent collision between the Yangtze and North China cratons in the Triassic followed by a continental extension led to the transformation of the regional tectonic regime from early (T_2-T_3) compression to late (J_3-K_1) extension and fault depression (Li, 1992), and resulted in a regional magmatic activity of alkali-olivine basalts. The alkali-olivine basaltic magma was derived from the upper mantle as deep as 45 km or more, and underplated at a depth of 27–35 km at about 140 Ma. After this, crystalline fractionation of the underplated alkali-olivine basaltic magma combined with assimilation of it with the lower crust attributed to the formation of the pyroxene and hornblende megacrysts and pyroxene and hornblende cumulates.

The following conclusions can be drawn for this study.

(1) An alkali-olivine basalt magma underplating took place at about 140 Ma in the Tongling region, Anhui Province.

(2) The pyroxene and hornblende megacrysts and cumulates in Tongling were formed through crystalline fractionation of the underplated alkali-olivine basaltic magma combined with the assimilation with the lower crust at depths of 27 km to 35 km.

Acknowledgements

This study was financially supported by the National Natural Science Foundation of China (Grants 40272034 and 40133020), the Ministry of Science and Technology of China (Grant 1999043206) and the Korea Science and Engineering Foundation (Grant KOSEF-20005-131-03-02). Senior Engineers Chu Guozheng, Zhang Chenghuo and Liu Guanghua provided invaluable assistance with the fieldwork. The comments of Academician Wang Dezi and the suggestions given by Prof. Zhou Xinmin, Kert Freihauf and Fan Qicheng led to great improvements on the manuscript.

Manuscript received March 20, 2003
accepted Jan. 18, 2004
edited by Liu Xinzhu

References

Best, M.G., 1974. Mantle-derived amphibole within inclusions in alkali basaltic lavas. *Journal of Geophysical Research*, 79: 2107–2113.

Chen Husheng, 1988. Outline of comprehensive demonstration for geophysical and geological data from HQ-13 line in the Lower Yangtze Basin, Yangtze Metaplatform. In: Chen Husheng (ed.), *Papers on the Exploration of New Fields for Gas and Oil Surveying in South China* (Vol. 2). Beijing: Geologic Publishing House. 65–73 (in Chinese).

Chi Jishang (editor in chief), 1987. *The Study of Cenozoic Basalts and Upper Mantle Beneath Eastern China (attachment: kimberlites)*. Beijing: Geological Publishing House, 277 (in Chinese with English abstract).

Du Yangsong, Liu Jinhui, Qin Xinlong, Lou Yaer and Dou Jinlong, 2003. Progresses in magmatic underplating research. *Progress in Natural Science*, 13: 237–242 (in Chinese).

Fan Qicheng and Liu Ruoxin, 1996. The high-temperature granulitic xenoliths from Hannuoba basalts. *Chinese Science Bulletin*, 41(3): 235–238 (in Chinese).

Fan Qicheng, Liu Ruoxin, Li Huimin, Li Ni, Sui Jianli and Lin Zhuoran, 1998. Zircon chronology and REE geochemistry of granulite xenolith at Hannuoba. *Chinese Science Bulletin*, 43 (2): 133–137 (in Chinese).

Fan Qicheng, Sui Jianxin, Liu Ruoxin and Zhou Xinmin, 2001. Eclogite facies garnet pyroxenite at Hannuoba—new evidence for magmatic underplating. *Acta Petrologica Sinica*, 17(1): 1–6 (in Chinese with English abstract).

Hollister, L.S., Grissom, G.C., Peters, E.K., Stowell, H.H., and Gisson, V.B., 1987. Confirmation of the empirical correlation of Al in hornblende with pressure of solidification of calc-alkaline plutons. *American Mineralogist*, 72: 231–239.

IMA-CNMMN, 1997. Nomenclature of amphibole. *The Canadian Mineralogist*, 35: 219–246.

Qiu Jiaxiang and Zeng Guangce, 1987. Mineralogical chemistry and petrological significance of low pressure clinopyroxenes in Cenozoic basalts in East China. *Acta Petrologica Sinica*, 3(4): 1–9 (in Chinese with English abstract).

Qiu Jiaxiang, Wang renjing and Li Changnian, 1991. *Potassium-rich Volcanic Rocks in Wudalianchi-Keluo-Erkeshan*. Wuhan: China University of Geosciences Press, 219 (in Chinese with English).

Sachs, P.M., Hansteen, T.H., 2000. Pleistocene underplating and metasomatism of the lower continent crust: a xenolith study. *Journal of Petrology*, 41(3): 331–356.

Shao Jian, Han Qingjun, Zhang Liqiao and Mou Baolei, 1999. Discovery of the early Paleozoic xenoliths of cumulates in East Inner Mongolia. *Chinese Science Bulletin*, 44(5): 478–485.

Shao Jian, Han Qingjun and Li Huimin, 2000. Discovery of the early Mesozoic granulite xenoliths in North China Craton. *Science in China* (Series D), 30 (Supp.): 148–153.

Tang Yongcheng, Wu Yanchang, Chu Guozheng, Xing Fengming, Wang Yongmin, Cao Fenyang and Chang Yinfo, 1998. *Geology of Copper-Gold Polymetallic Deposits along the Yangtze River, Anhui Province.* Beijing: Geological Publishing House, 351 (in Chinese with English abstract).

Warren, R.G., Kudo, A.M., and Keil, K., 1979. Geochemistry of lithic and single-crystal inclusions in basalt and characterization of upper mantle-lower crust in the Engle basin, Rio Grande Rift, New Mexico. In: Riecker, R.E. (ed.). *Rio-Grande Rift: Tectonics and Magmatism.* Washington DC: American Geophysical Union, 393–415.

Wu Cailai, Zhou Xunruo, Huang Xuchen, Zhang Chenghuo, Xu Sheng, Guo Heping and Chen Siyou, 1997. Enclave petrology of intermediate-acidic intrusive rocks in Tongling district, Anhui. Acta *Geoscientia Sinica*, 18(2): 182–191 (in Chinese with English abstract).

Xia Jia, 1982. Petrology of volcanic rocks in Niutoushan, Fujian Province. *M. S. thesis of Wuhan College of Geology*, 64 (in Chinese).

Xing Fengming and Xu Xiang, 1996. High-potassium calc-alkaline intrusive rocks in Tongling area, Anhui Province. *Geochimica*, 25(1): 29–38 (in Chinese with English abstract).

Xing Fengming, Zhao Bin, Xu Xiang, Zhu Chengming, Zhao Jinsong and Cai Enzhao, 1997. Experimental study on the genesis of intrusive rocks in the Tongling area, Anhui. *Regional Geology*, 16(3): 267–274 (in Chinese with English abstract).

Xu Xisheng and Zhou Xinmin, 1995. The xenoliths from Qilin Cenozoic basaltic pipe, Guangdong. *Acta Petrologica Sinica*, 11(4): 441–448 (in Chinese with English abstract).

Ye Huiwen, 1992. Calculation of Fe^{3+} and Fe^{2+} in amphiboles. In: Zhang Yixia, Lu Liangzhao, Yan Hongquan and Xu Xuechun (eds.), *Collected Works of Institute of Geology, Changchun College of Geology.* Beijing: Seismological Press. 63–74 (in Chinese with English abstract).

Yu Jinhai, Fang Zhong, Lai Mingyuan, Zhou Xinmin, Luo Shuwen and Zhou Xuan, 1998. Discovery of garnet granulite facies xenoliths in Cenozoic basalts, Leizhou, Guangdong Province. *Chinese Science Bulletin*, 43(18): 1988–1991 (in Chinese).

Yu Jinhai, Xu Xisheng and Zhou Xinmin, 2002. Late Mesozoic crust-mantle interaction and lower crust components in SE China: a geochemical study of mafic granulite xenoliths from Cenozoic basalts. *Science in China* (Series D), 32(5): 383–393 (in Chinese).

Zheng Jianping, Sun Min, Lu Fengxiang, Wang Chunyang and Zhong Zengqiu, 2001. Garnet-bearing granulite faces rock xenoliths from Late Mesozoic volcaniclastic breccia, Xinyang, Henan Province. *Acta Geologica Sinica* (English edition), 75 (4): 445–451.

Zheng Qiaorong, 1984. Calculation of Fe^{3+} and Fe^{2+} from electronprobe analyzing data. *Acta Mineralogica Sinica*, 4(1): 55–62 (in Chinese with English abstract).

Zhou Xinmin, Yu Jinhai and Xu Xisheng, 1992. Granulite xenoliths from Nüshan basalts. *Chinese Science Bulletin*, 37 (13): 1198–1201 (in Chinese).

Zhou Xunruo, Wu Cailai, Huang Xuchen and Zhang Chenghuo, 1993. Characteristics of cognate inclusions in intermediate-acid intrusive rocks of Tongling area and their magmatic danamics. *Acta Petrologica et Mineralogica*, 12(1): 20–31 (in Chinese with English abstract).